

Minority Carrier Lifetime Measurements by Photoinduced Carrier Microwave Absorption Method

Toshiyuki Sameshima*, Tomokazu Nagao, Shinya Yoshidomi, Kazuya Kogure, and Masahiko Hasumi

Tokyo University of Agriculture and Technology, Koganei, Tokyo 184-8588, Japan

Received July 8, 2010; accepted September 7, 2010; published online March 22, 2011

We propose a measurement system for photoinduced minority carrier absorption of 9.35 GHz microwaves using periodically pulsed light illumination at 620 nm. The ratio of average carrier density when light illumination is ON to that when light illumination is OFF, P , was theoretically analyzed for different light pulse widths. The analysis of P resulted in a formula giving the minority carrier lifetime τ_{eff} of silicon under continuous light illumination. τ_{eff} for holes was experimentally determined using the formula, and its spatial distribution was obtained to be from 1.0×10^{-3} to 1.28×10^{-3} s for n-type silicon substrates with a thickness of 520 μm coated with 100-nm-thick thermally grown SiO_2 layers. We also demonstrated that τ_{eff} depended on the means of light illumination for a defective sample. Two different τ_{eff} values were obtained, 7×10^{-5} and 1.73×10^{-4} s, in the cases of light illumination to the top surface and rear surface, respectively, when the SiO_2 layer was etched up to 2 nm at the top surface. © 2011 The Japan Society of Applied Physics

1. Introduction

Semiconductor solar cells have been attractive as a device producing electrical power from sunlight.^{1,2)} A high quality of semiconductors and their surfaces is demanded for achieving a high conversion efficiency of such cells. The analysis of the photoinduced carrier properties of semiconductors is therefore important. A nondestructive and noncontact measurement system is attractive for such a purpose. Measurements of quasi-steady-state photoconductance (QSSPC) and microwave photoconductive decay have been widely used for the measurement of the photoinduced minority carrier lifetime.³⁻⁸⁾ Precise analysis of photoconductive decay characteristics has been established using a free-carrier diffusion process in order to investigate the minority carrier surface recombination velocity as well as the minority carrier bulk lifetime, which are important parameters for evaluating the photoconductive properties of semiconductors.⁹⁻¹¹⁾ When surfaces are well passivated and surface recombination velocities are sufficiently low, the effective lifetime $\tau_{\text{classical}}$ is directly given by the minority bulk carrier lifetime τ_b , the minority carrier recombination velocities of the top and rear surfaces, S_{top} and S_{rear} , respectively and the substrate thickness d . $\tau_{\text{classical}}$ is independent of the carrier diffusion coefficient. A well-known and simple description of $\tau_{\text{classical}}$ has been widely used:¹²⁾

$$\tau_{\text{classical}} = \left(\frac{1}{\tau_b} + \frac{S_{\text{top}}}{d} + \frac{S_{\text{rear}}}{d} \right)^{-1}. \quad (1)$$

We have developed a microwave free-carrier absorption measurement system with continuous-wave (CW) light illumination.¹³⁾ The free-carrier absorption effect is sensitive in the microwave frequency region. Free carriers in semiconductors respond to the incident electrical field of microwaves on the order of GHz and complex refractive indexes can be changed so that the transmissivity changes with the density of free carriers. The change in microwave transmittance precisely gives the density of minority carriers. When CW light is illuminated to a semiconductor sample, the density of minority carriers per unit area, N , is effectively given by the carrier generation rate G per unit area, determined by photon flux, internal quantum efficiency, and light reflection loss, and the effective minority carrier lifetime $\tau_{\text{eff}}^{\text{CW}}$ as

$$N = \tau_{\text{eff}}^{\text{CW}} G. \quad (2)$$

$\tau_{\text{eff}}^{\text{CW}}$ is governed by carrier annihilation via the recombination of holes and electrons in defect states located at the surfaces of a semiconductor as well as in its bulk. In previous reports,^{13,14)} we analyzed $\tau_{\text{eff}}^{\text{CW}}$ in the case of carrier generation occurred just at the semiconductor surface as

$$\tau_{\text{eff}}^{\text{CW}} = \tau_b \frac{\sqrt{\frac{D}{\tau_b}} \left[1 - \exp\left(-\frac{d}{\sqrt{D\tau_b}}\right) \right] \left[\sqrt{\frac{D}{\tau_b}} + S_{\text{rear}} + \left(\sqrt{\frac{D}{\tau_b}} - S_{\text{rear}} \right) \exp\left(-\frac{d}{\sqrt{D\tau_b}}\right) \right]}{\left(\sqrt{\frac{D}{\tau_b}} + S_{\text{rear}} \right) \left(\sqrt{\frac{D}{\tau_b}} + S_{\text{top}} \right) - \left(\sqrt{\frac{D}{\tau_b}} - S_{\text{top}} \right) \left(\sqrt{\frac{D}{\tau_b}} - S_{\text{rear}} \right) \exp\left(-\frac{2d}{\sqrt{D\tau_b}}\right)}, \quad (3)$$

where D is the minority carrier diffusion coefficient and S_{top} is the surface recombination velocity on the light illumination side (top surface). S_{rear} is the recombination velocity on the dark side (rear surface). N was precisely measured with a limitation on the order of 10^{10} cm^{-2} by detecting the change in microwave intensity with sufficient integration time under CW light illumination. This is an advantage for the investigation of the low carrier generation rate associated

with a low light intensity. However, it is not easy to experimentally determine $\tau_{\text{eff}}^{\text{CW}}$ under CW light illumination because the carrier generation rate G strongly depends on light reflection loss, which is sometimes unknown. A transient measurement system is therefore important to obtain the minority carrier lifetime.

In this paper, we propose a free-carrier microwave absorption measurement system with periodically pulsed light illumination, which precisely gives the effective minority carrier lifetime τ_{eff} under a low light intensity.

*E-mail address: tsamesim@cc.tuat.ac.jp

The ratio of the average carrier density in the dark to that under light illumination, P , is measured by time integration during illumination with many light pulses. The analysis of P gives a formula for determining τ_{eff} , which is close to $\tau_{\text{eff}}^{\text{CW}}$. We discuss carrier annihilation properties using P and τ_{eff} . We demonstrate the measurement of τ_{eff} using the present method without information on G for n-type crystalline silicon.

2. Theory

We supposed that photoinduced carriers were annihilated at recombination sites concentrated at the surfaces and uniformly distributed in the bulk substrate. The recombination sites at the surfaces give the surface recombination velocities S_{top} and S_{rear} . The recombination sites uniformly distributed in the bulk substrate gave the bulk lifetime τ_b . When light is absorbed in the top surface region of semiconductors with a sufficiently high absorption coefficient, the generation of photoinduced carriers is limited just in the top surface region, while there is no carrier generation in the bulk. The photoinduced minority carriers therefore diffuse into the substrate according to time-dependent diffusion equation¹⁵⁾ as,

$$D \frac{\partial^2 n(x, t)}{\partial x^2} - \frac{n(x, t)}{\tau_b} = \frac{\partial n(x, t)}{\partial t}, \quad (4)$$

where $n(x, t)$ is the carrier volume density at a depth of x and at a time of t . Carrier generation and carrier annihilation occur at the top surface, and carrier annihilation only occurs at the rear surface. We therefore place the boundary conditions of carrier generation and carrier recombination ratios as

$$D \left. \frac{\partial n(x, t)}{\partial x} \right|_{x=0} = S_{\text{top}} n(0, t) - G(t), \quad (5a)$$

$$D \left. \frac{\partial n(x, t)}{\partial x} \right|_{x=d} = -S_{\text{rear}} n(d, t), \quad (5b)$$

where D is the diffusion constant of minority carriers, $G(t)$ is the carrier generation ratio per unit area determined by photon flux, internal quantum efficiency, and light reflection loss, and d is the thickness of the semiconductor substrate. $n(x, t)$ was calculated using a time-evolution-type finite element differential method when light is periodically illuminated for a duration of T , and light is subsequently turned off for T , as shown in Fig. 1(a). For the finite element calculation, the lattice constant should be much lower than the carrier diffusion length for the minimum light pulse width or minimum bulk lifetime. Since the minimum light pulse width and minimum bulk lifetime were 2.5 and 10 μs in this paper, those carrier diffusion lengths were about 55 and 110 μm , respectively. The lattice constant was set at 2 μm , which was similar to the light penetration depth shown in the Experimental Procedure. The minority carrier density

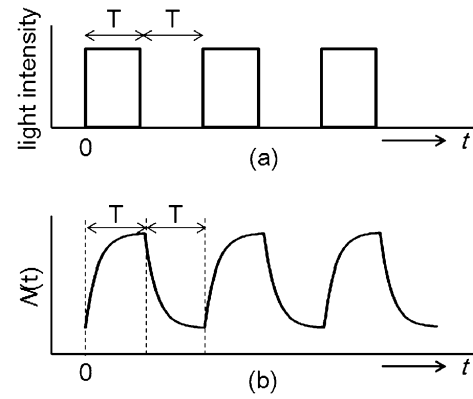


Fig. 1. Images of light illumination (a), and generation and annihilation of photoinduced carriers (b).

per unit area $N(t)$ was also calculated by integrating $n(x, t)$ with x from 0 to d at each t as

$$N(t) = \int_0^d n(x, t) dx. \quad (6)$$

$N(t)$ changes with time as shown in Fig. 1(b). $N(t)$ increases under light illumination and decreases in the dark. It is essential that $N(t)$ must periodically change according to periodic light illumination after sufficient time from the initiation of illumination. $N(t)$ consists of zero-frequency (CW) components, which include information on $\tau_{\text{eff}}^{\text{CW}}$, as well as components of integral multiples of the fundamental frequency of $0.5T^{-1}$. The minimum calculation cycle number m for obtaining periodic $N(t)$ was defined as

$$\frac{|N(2mT) - N(2(m-1)T)|}{N(2mT)} < 0.001. \quad (7)$$

Time zero ($t = 0$) was defined again after $2mT$ in order to calculate periodic $N(t)$ when the light is ON and when the light is OFF. The average carrier density during light illumination, N_{on} , was calculated by time integration from 0 to T . The average density of residual carriers in the dark (light OFF), N_{off} , was also obtained by time integration from T to $2T$. We defined $P(T)$ as the ratio of $N_{\text{off}}/N_{\text{on}}$ as

$$P(T) = \frac{N_{\text{off}}}{N_{\text{on}}} = \frac{\frac{1}{T} \int_T^{2T} N(t) dt}{\frac{1}{T} \int_0^T N(t) dt}. \quad (8)$$

We calculated $P(T)$ as a function of T with different τ_b , S_{top} , and S_{rear} values in the cases of minority carriers of holes and electrons.

When S_{top} and S_{rear} were 0, $N(t)$ was simply expressed using a model with a single time constant τ_b because the carrier annihilation ratio was governed by τ_b at any spatial points in the substrate as

$$N(t) = \begin{cases} G\tau_b \left(1 - \exp\left(-\frac{t}{\tau_b}\right) \right) + G\tau_b \frac{\exp(-T/\tau_b)}{1 + \exp(-T/\tau_b)} \exp\left(-\frac{t}{\tau_b}\right) & (0 < t < T), \\ G\tau_b \frac{\exp(T/\tau_b)}{1 + \exp(-T/\tau_b)} \exp\left(-\frac{t}{\tau_b}\right) & (T < t < 2T). \end{cases} \quad (9)$$

$P(T)$ was given as

$$P(T) = \frac{N_{\text{off}}}{N_{\text{on}}} = \frac{(\tau_b/T)[1 - \exp(-T/\tau_b)]}{1 + \exp(-T/\tau_b) - (\tau_b/T)[1 - \exp(-T/\tau_b)]}. \quad (10)$$

$P(T)$ monotonically decreased from 1 to 0 as T increased. When $T = \tau_b$, $P(T)$ was expressed as

$$P(\tau_b) = \frac{e - 1}{2} \sim 0.859. \quad (11)$$

When light pulses with a width of τ_b were periodically illuminated, most of the minority carriers remained in the semiconductor in the dark in the case of S_{top} and S_{rear} of 0. When T was $2\tau_b$, $P(T)$ was expressed as

$$P(2\tau_b) = \frac{1 - e^{-2}}{1 + 3e^{-2}} \sim 0.615. \quad (12)$$

$P(T)$ decreased from 0.859 to 0.615 as T increased from τ_b to $2\tau_b$. We designated the pulse width for $P(T)$ at 0.859 as τ_{pulse} in general cases it was expressed as

$$\tau_{\text{pulse}} = T(P = 0.859). \quad (13)$$

Moreover, we defined R as the time difference between pulse widths for $P(T)$ at 0.615 and 0.859 divided by the pulse width for $P(T)$ at 0.859 as

$$R = \frac{T(P = 0.615) - T(P = 0.859)}{T(P = 0.859)}. \quad (14)$$

τ_{pulse} and R were τ_b and 1, respectively, in the limited case of S_{top} and S_{rear} of 0. τ_{pulse} and R were used to characterize minority carrier annihilation properties and obtain the effective minority carrier lifetime for the present method.

According to the free-carrier absorption model,¹³⁾ the photoinduced carrier volume density $n(x, t)$ causes a change in complex specific dielectric constant. The real part ϵ_r and the imaginary part ϵ_i of the complex specific dielectric constant of semiconductor are expressed as

$$\epsilon_r = n_f^2 - k_f^2 = \epsilon^* \left(1 - \frac{\omega_p^2 \tau^2}{1 + \omega^2 \tau^2} \right), \quad (15)$$

$$\epsilon_i = 2n_f k_f = \epsilon^* \frac{\omega_p^2 \tau}{\omega(1 + \omega^2 \tau^2)}, \quad (16)$$

where ω is the angular frequency, ϵ^* is the specific dielectric constant of the semiconductor in the dark, n_f is the refractive index of the semiconductor, k_f is the extinction coefficient of the semiconductor, τ is the motion lifetime of free carriers, and ω_p is the plasma angular frequency expressed as

$$\omega_p = \sqrt{\frac{e^2 n(x, t)}{m^* \epsilon_0 \epsilon^*}}, \quad (17)$$

where ϵ_0 is the dielectric constant in vacuum, e is the elemental charge and m^* is the effective mass of free carriers. The refractive index and extinction coefficient are given with the real part ϵ_r and the imaginary part ϵ_i of ϵ as

$$n = \sqrt{\frac{\epsilon_r + \sqrt{\epsilon_r^2 + \epsilon_i^2}}{2}}, \quad (18)$$

$$k = \frac{\epsilon_i}{\sqrt{2} \sqrt{\epsilon_r + \sqrt{\epsilon_r^2 + \epsilon_i^2}}}, \quad (19)$$

The absorption coefficient α is given as

$$\alpha = \frac{4\pi k}{\lambda} = \frac{\sqrt{2} \omega \epsilon_i}{c \sqrt{\epsilon_r + \sqrt{\epsilon_r^2 + \epsilon_i^2}}}, \quad (20)$$

where c is the light velocity. A semiconductor solid has a serious damping property with a short motion lifetime less than 10^{-12} s. In this case, α was approximately expressed as

$$\alpha \sim \frac{\omega_p^2 \tau}{c \sqrt{1 - \omega_p^2 \tau^2}} \sim \frac{en(x, t)\mu}{\epsilon_0 \epsilon_c^*}, \quad (21)$$

where μ is the carrier mobility. When α is not so large, the microwave transmittance T_r is expressed as

$$\frac{d}{dx} \left(\frac{T_r}{T_{r0}} \right) = -\alpha \left(\frac{T_r}{T_{r0}} \right) \sim -\frac{e\mu}{\epsilon_0 \epsilon_c^*} \left(\frac{T_r}{T_{r0}} \right) n(x, t), \quad (22)$$

where T_{r0} is the microwave transmittance in the dark field. The integration of eq. (22) with depth gave a simple relation between transmittance and carrier density per unit area $N(t)$ defined by eq. (6) as

$$\ln \left(\frac{T_r}{T_{r0}} \right) \sim -\frac{e\mu}{\epsilon_0 \epsilon_c^*} \int_0^d n(x, t) dx = -CN(t), \quad (23)$$

$$N(t) \sim \frac{\ln T_{r0} - \ln T_r}{C},$$

where C is a constant of $e\mu/(\epsilon_0 \epsilon_c^*)$. $P(T)$, defined by eq. (8), is therefore experimentally obtained using the logarithm of the microwave transmittance as

$$P(T) = \frac{\int_T^{2T} (\ln T_{r0} - \ln T_r) dt}{\int_0^T (\ln T_{r0} - \ln T_r) dt}. \quad (24)$$

3. Experimental Procedure

Two 15 Ω cm n-type 4-in. silicon substrates with a thickness of 520 μm were prepared. The both surfaces of both substrates were coated with 100-nm-thick thermally grown SiO_2 layers (sample I). The SiO_2 layer at the top surface of a silicon substrate was thinned to about 2 nm using 5% diluted hydrofluoric acid to make a defective surface with a high surface recombination velocity at the top surface (sample II).

The 9.35 GHz microwave transmittance measurement system was constructed using waveguide tubes, as shown in Fig. 2. It had a narrow gap for placing a sample wafer. A small hole was opened on a wall of the waveguide to place an optical fiber for introducing light from a 620 nm light-emitting diode (LED). Crystalline silicon has an optical absorption coefficient of 4460 cm^{-1} at 620 nm.¹⁶⁾ The optical penetration depth was therefore about 2.2 μm , which was much lower than the substrate thickness. Carrier generation was limited in the surface region. The light was switched by switching the operation voltage applied to the diode with pulse widths ranging from 5×10^{-5} to 1×10^{-2} s. A Teflon plate was placed aslant in the waveguide tube to reflect and diffuse LED light. Consequently, the sample was uniformly

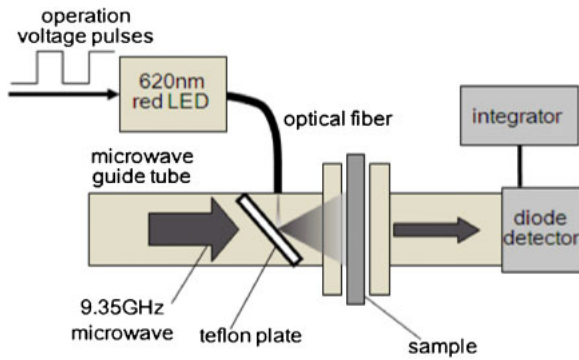


Fig. 2. (Color online) Schematic of experimental apparatus.

illuminated at 0.8 mW/cm^2 with periodic LED light pulses. Microwave was coincidentally switched with the light pulse turned ON or OFF, respectively, using a coincident switching circuit to obtain changes in microwave transmittance during light ON or OFF. The microwave, which transmitted the sample, was rectified using a high-speed diode and integrated with time with a time constant of 2 s. The integrated voltage was detected by a digital electrometer. The change in the transmittance of microwaves was also measured in the case of CW light illumination for comparison.

4. Results and Discussion

Figure 3 shows the calculated $P(T)$ as a function of T for the hole minority carrier for the 520- μm -thick silicon substrate in cases of τ_b (s), S_{top} (cm/s), and S_{rear} (cm/s) as follows: A: 1×10^{-5} , 0, 0, B: 1, 0, 5200, C: 1, 5200, 0, D: 1, 2600, 2600 (a) and E: 4×10^{-4} , 0, 0, F: 1, 0, 130, G: 1, 130, 0, and H: 1, 65, 65 (b), respectively. The $\tau_{\text{classical}}$ values were 1×10^{-5} s in the four cases shown in Fig. 3(a) and 4×10^{-4} s in the four cases shown in Fig. 3(b), respectively. $P(T)$ was high at almost 1 when T was shorter than 1×10^{-5} s in every case, as shown in Fig. 3(a). This means that the average carrier densities were almost the same between the light ON and OFF states because light switching was sufficiently rapid compared with the carrier annihilation. $P(T)$ monotonically decreased as T increased. The average carrier density during light OFF was lower than that during light ON when T was long because minority carriers annihilated during a long dark duration. The change in $P(T)$ with T was simply described by a single time constant of 1×10^{-5} s in case A, as given in eq. (10). On the other hand, $P(T)$ remained constant at 1 up to a T of 7×10^{-5} s in case B as shown in Fig. 3(a) because minority carriers were alive up to the time of diffusion from the top surface to the rear surface with a diffusion coefficient of $12 \text{ cm}^2/\text{s}$ for holes. $P(T)$ then rapidly decreased as T increased from 7×10^{-5} s, as shown in Fig. 3(a). There was sufficient time for carriers to reach and annihilate at the rear surface in the dark. The characteristic of $P(T)$ in case B was much different from that in case A, as shown in Fig. 3(a), although both conditions gave the same $\tau_{\text{classical}}$ of 1×10^{-5} s. On the other hand, $P(T)$ gradually decreased as T increased in the case of the defective top surface, C, as shown in Fig. 3(a). Photoinduced carriers effectively annihilated at the surface for all pulse widths. However, some carriers diffused into the substrate and remained alive for a long time until their diffusion back to the top surface

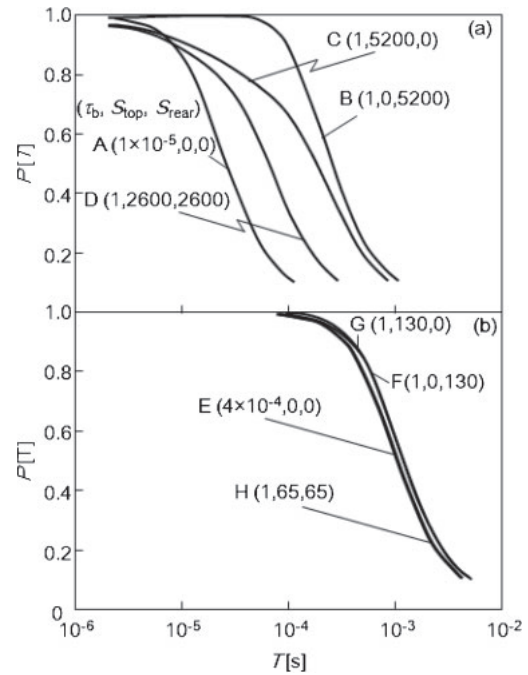


Fig. 3. Calculated $N(t)$ as a function of T for the hole minority carriers for 520- μm -thick silicon substrate in cases of τ_b (s), S_{top} (cm/s), S_{rear} (cm/s) as follows: A: 1×10^{-5} , 0, 0, B: 1, 0, 5200, C: 1, 5200, 0, D: 1, 2600, 2600 (a) and as, E: 4×10^{-4} , 0, 0, F: 1, 0, 130, G: 1, 130, 0, and H: 1, 65, 65 (b), respectively. The $\tau_{\text{classical}}$ values were 1×10^{-5} s in the cases A–D in (a) and 4×10^{-4} s in cases E–H in (b).

because there was almost no defect in the bulk or at the rear surface. $P(T)$ was therefore rather high in the large-pulse-width case. Case D gave defects equivalently located at both surfaces. Photoinduced carriers annihilate at the top surface as well as at the rear surface. It was similar to case C at half of the substrate thickness. $P(T)$ was therefore lower than that in case C. The results of cases A to D shown in Fig. 3(a) indicate that the present method can be used for analyzing defect localization. On the other hand, the $P(T)$ characteristics were similar among cases E to H, as shown in Fig. 3(b). $\tau_{\text{classical}}$ was 4×10^{-4} s, given by a long τ_b , a low S_{top} , and a low S_{rear} . These results come from the fact that a low carrier annihilation rate gives a similar density of photoinduced carriers and its in-depth distribution for all defect localization types. In low-carrier-annihilation cases, $\tau_{\text{classical}}$ has an effect on what and defect localization cannot be distinguished.

Figure 4 shows a summary of $P(T)$ for hole minority carriers as a function of T in cases of τ_b values ranging from 1×10^{-5} to 1×10^{-3} s, and $S_{\text{top}} = S_{\text{rear}} = 0$ (a); $\tau_b = 1$ s, $S_{\text{top}} = 0$, and S_{rear} values ranging from 5200 to 52 cm/s (b); $\tau_b = 1$ s, S_{top} values ranging from 5200 to 52 cm/s, and $S_{\text{rear}} = 0$ (c); and $\tau_b = 1$ s, and $S_{\text{top}} = S_{\text{rear}}$ values ranging from 2600 to 26 cm/s (d). The 15 conditions of τ_b , S_{top} , and S_{rear} in each case gave the same $\tau_{\text{classical}}$ series ranging from 1×10^{-5} to 1×10^{-3} s, the same as that given in case (a). $P(T)$ monotonically decreased as T increased for every case because the average density of residual carriers in the dark decreased as the duration of light OFF increased. Similar $P(T)$ shapes were obtained among Figs. 4(a)–4(d) cases for $\tau_{\text{classical}}$ longer than 4×10^{-4} s. This means that the carrier concentrations were similar and similarly distributed in the

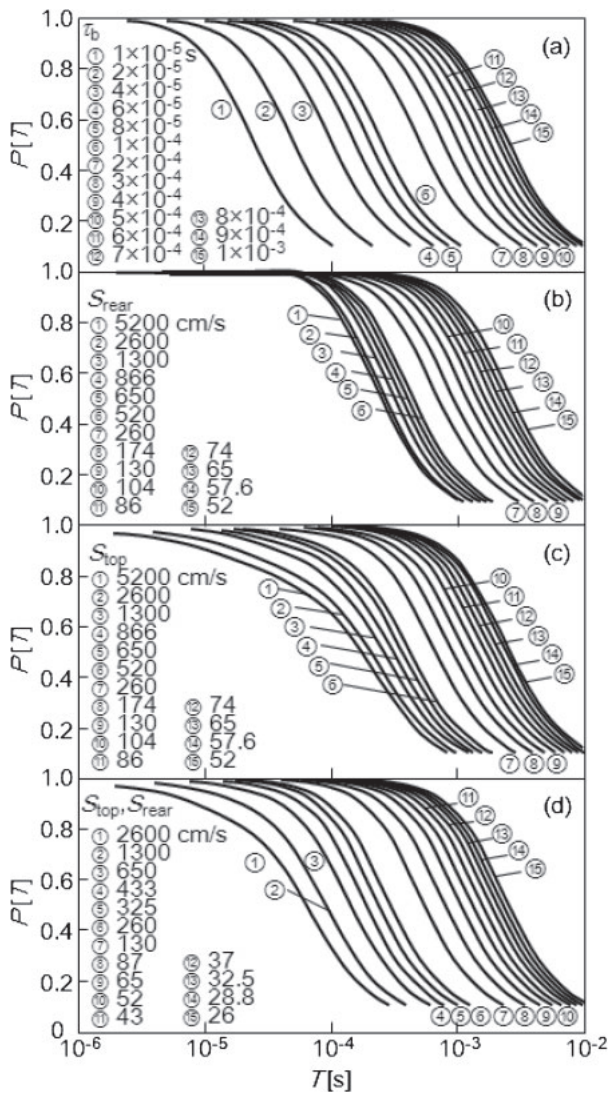


Fig. 4. $N(t)$ for hole minority carriers as function of T in cases of τ_b values ranging from 1×10^{-5} to 1×10^{-3} s, and $S_{top} = S_{rear} = 0$ (a); $\tau_b = 1$ s, $S_{top} = 0$, and S_{rear} values ranging from 5200 to 52 cm/s (b); $\tau_b = 1$ s, S_{top} values ranging from 5200 to 52 cm/s; and $S_{rear} = 0$ (c), and $\tau_b = 1$ s, and $S_{top} = S_{rear}$ values ranging from 2600 to 26 cm/s (d).

depth direction among cases (a)–(d), and that τ_b^{-1} , S_{top}/d , and S_{rear}/d equally contributed carrier annihilation properties in the four carrier annihilation cases. On the other hand, different $P(T)$ behaviors were obtained among cases (a)–(d) for $\tau_{classical}$ shorter than 4×10^{-4} s. In the case shown in Fig. 4(a), the $P(T)$ shape plotted as a function of logarithmic T was the same for every τ_b ($= \tau_{classical}$) because $P(T)$ is governed by τ_b/T , as shown in eq. (10). On the other hand, $P(T)$ curves shifted to long- T regions for the first 8 conditions with S_{rear} values ranging from 5200 to 174 cm/s for $\tau_{classical}$ less than 4×10^{-4} s, as shown in Fig. 4(b) compared with Fig. 4(a). Photoinduced minority carriers remained for a long time until their diffusion to the rear surface. On the other hand, in the case shown in Fig. 4(c), $P(T)$ gradually decreased in the short- T regions, and the low- $P(T)$ regions shifted to the high- T regions under the first 8 conditions with S_{top} values ranging from 5200 to 174 cm/s for $\tau_{classical}$ less than 4×10^{-4} s, compared with Fig. 4(a). The density of photoinduced minority carriers was effectively decreased by high S_{top} for all pulse widths. On

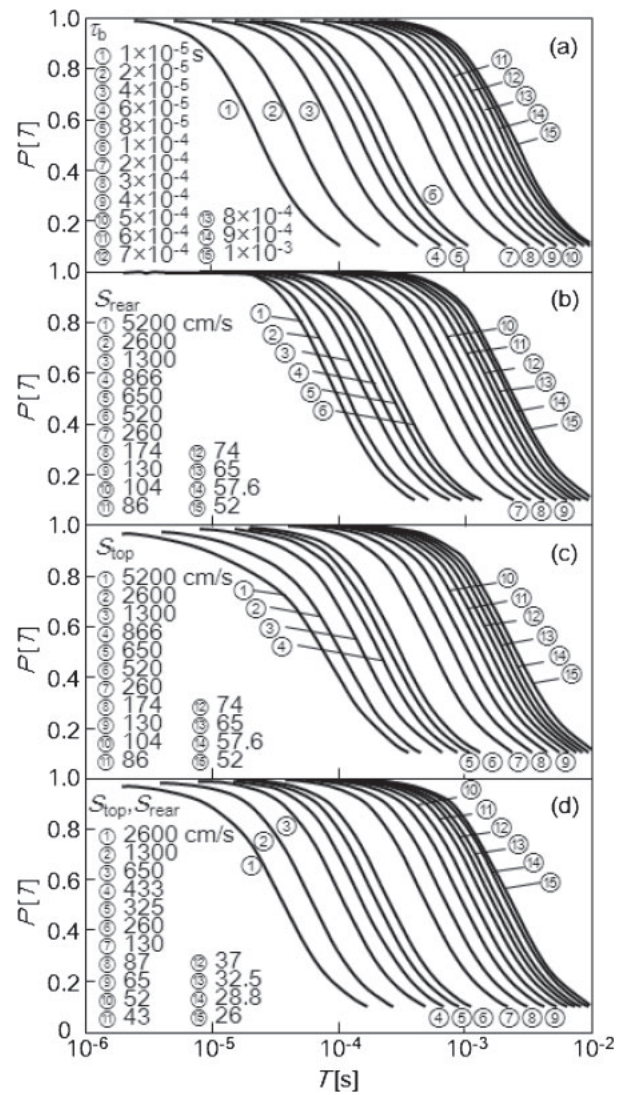


Fig. 5. $N(t)$ for the electron minority carrier as function of T for cases of τ_b values ranging from 1×10^{-5} to 1×10^{-3} s, and $S_{top} = S_{rear} = 0$ (a); $\tau_b = 1$ s, $S_{top} = 0$, and S_{rear} values ranging from 5200 to 52 cm/s (b); $\tau_b = 1$ s, S_{top} values ranging from 5200 to 52 cm/s; and $S_{rear} = 0$ (c), and $\tau_b = 1$ s, and $S_{top} = S_{rear}$ values ranging from 2600 to 26 cm/s (d).

the other hand, when they diffused into the silicon bulk, they were alive until their diffusion back to the top surface. The same recombination velocity at the top and rear surfaces and a long bulk lifetime of 1 s resulted in $P(T)$ characteristics between the cases shown in Figs. 4(a) and 4(c). The minority carriers that diffused into the silicon bulk could be annihilated at the rear surface before returning to the top surface. This was effectively equivalent to the thin substrate condition shown in Fig. 4(c). A close localization of defects means an effectively uniform distribution of defects.

We also calculated the $P(T)$ characteristics of electron minority carriers. Figures 5(a)–5(d) show a summary of $P(T)$ values for the electron minority carrier as functions of T under the same conditions of τ_b , S_{top} , and S_{rear} given in Figs. 4(a)–4(d) for hole minority carriers. In the cases of τ_b values ranging from 1×10^{-5} to 1×10^{-3} s, and $S_{top} = S_{rear} = 0$ (a), $P(T)$ gave the completely the same results as those for hole minority carriers, as shown in Figs. 4(a) and 5(a) because there was a uniform annihilation rate given by τ_b in the silicon bulk. Although the $P(T)$ values in the

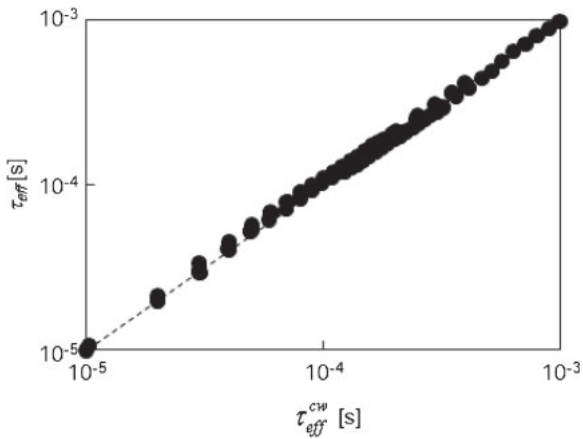


Fig. 6. τ_{eff} as a function of $\tau_{\text{eff}}^{\text{CW}}$ in four defect localization cases shown in Figs. 3–5.

other three cases also gave similar results to those for hole minority carriers, as shown in Figs. 4(b)–4(d) and 5(b)–5(d), the $P(T)$ behaviors in cases (b) to (d) for electron minority carriers were similar each other compared with those in case (a) than to those for hole minority carriers. Electrons have a high diffusion coefficient of $36 \text{ cm}^2/\text{s}$ compared with $12 \text{ cm}^2/\text{s}$ for holes. The high diffusivity increased the minority carrier diffusion length so that electrons more effectively interacted with defects located spatially apart than holes.

The effective carrier lifetime was obtained by the analysis of $P(T)$ values shown in Figs. 3–5. Through many numerical investigations, we propose the effective carrier lifetime τ_{eff} as

$$\tau_{\text{eff}} = \frac{\tau_{\text{pulse}}}{1 + \log R}. \quad (25)$$

τ_{eff} was equivalent to $\tau_{\text{classical}}$ under a limited condition of $S_{\text{top}} = S_{\text{rear}} = 0$. In this case, $P(T)$ was governed by τ_b under as given by eq. (10). τ_{pulse} was τ_b equivalent to $\tau_{\text{classical}}$, as given by eqs. (1) and (13). R was 1 under this condition as given by eq. (14). In other cases, especially highly defective surfaces, τ_{pulse} was not equivalent to $\tau_{\text{classical}}$, as shown in Fig. 3. Figure 6 shows τ_{eff} as a function of $\tau_{\text{eff}}^{\text{CW}}$ in the four defect localization cases shown in Figs. 3–5. There was a very good agreement between these cases from 1×10^{-5} to 10^{-3} s. The difference between them was less than 15% of their values. This indicates that τ_{eff} defined in eq. (25) gives the minority carrier lifetime under CW light illumination. The advantage of the present method of microwave transmission measurement under periodically pulsed light illumination is that no information of the carrier generation rate G is necessary. Therefore, the present method can be applied to the measurement of the minority carrier lifetime for sample with a complicated surface structure with no information on surface reflectivity. Figure 7 shows R as a function of τ_{eff} for the hole minority carrier (a) and the electron minority carrier (b) in the four defect cases shown in Figs. 4 and 5. R was only 1 in the case of $S_{\text{top}} = S_{\text{rear}} = 0$. On the other hand, it was higher than 1 when the top surface was defective with high recombination velocities, as shown in Figs. 4(c) and 5(c), because $N(t)$ gradually decreased as T increased. R was lower than 1 when the rear surface was defective with high recombination velocities, as shown in

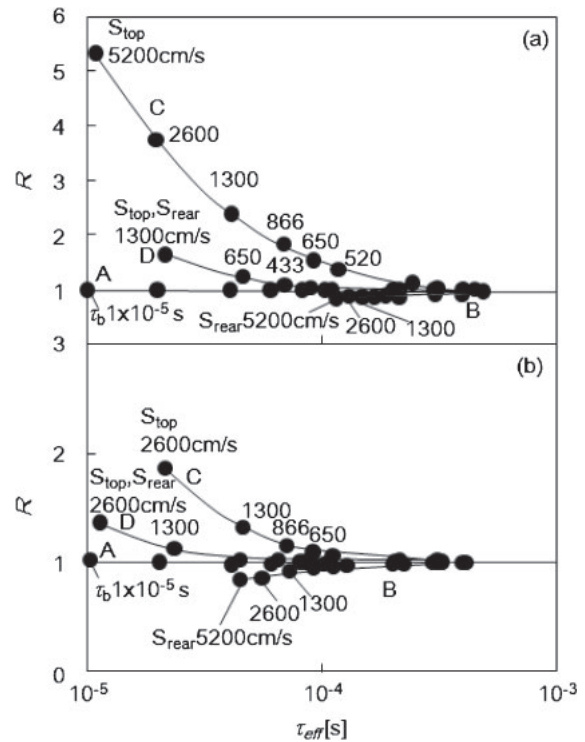


Fig. 7. R as a function of τ_{eff} for hole minority carriers (a) and electron minority carriers (b) in four defect cases shown in Figs. 4 and 5.

Figs. 4(b) and 5(b), because $P(t)$ was high for T at least up to the time of carrier diffusion across the substrate thickness and then rapidly decreased as T further increased. R became 1 as τ_{eff} exceeded 4×10^{-4} s for hole minority carriers and 2×10^{-4} s for the electron minority carriers, as shown in Figs. 7(a) and 7(b), respectively. τ_{eff} was equivalent to $\tau_{\text{classical}}$. Therefore, $\tau_{\text{classical}}$ has an effect on when it is above 4×10^{-4} s for hole minority carriers and 2×10^{-4} s for electron minority carriers, which is realized using good-quality silicon with a long τ_b , a low S_{top} , and a low S_{rear} . On the other hand, $\tau_{\text{classical}}$ cannot be used for defective materials. R depends on defect localization and its density. τ_{eff} gives an accurate effective lifetime over a wide range of carrier recombination densities for CW light illumination. R for hole minority carriers can have a very high values compared with R for electron minority carriers, as shown in Fig. 7. This is because of the low carrier diffusivity. Defect localization can seriously affect photoinduced hole carrier annihilation properties.

Figure 8 shows experimental $P(T)$ as a function of T for measurements at different places of sample I. The measurements were carried out by moving sample I in the horizontal and vertical directions normal to the incident microwave in steps of 10 mm in the horizontal direction and in steps of 5 mm in the vertical direction using a moving stage. The measurements at different places resulted in similar $P(T)$ curves, which were functions of T with single time constants given by eq. (10). $N(t)$ was almost 1 for T up to 3×10^{-4} s. These indicate that sample I had long effective minority carrier lifetimes, which distributed rather uniformly over the substrate. Figure 9 shows the τ_{eff} spatial distribution analyzed from $P(T)$ shown in Fig. 8 by eq. (25). τ_{eff} ranged from 1.0×10^{-3} to 1.28×10^{-3} s. It was obtained with a

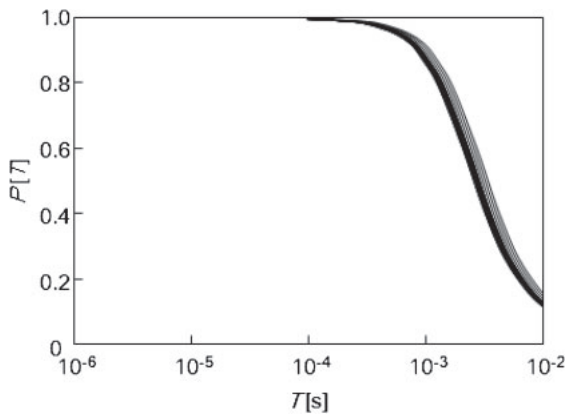


Fig. 8. Experimental $P(t)$ as a function of T for measurement at different places of sample I.

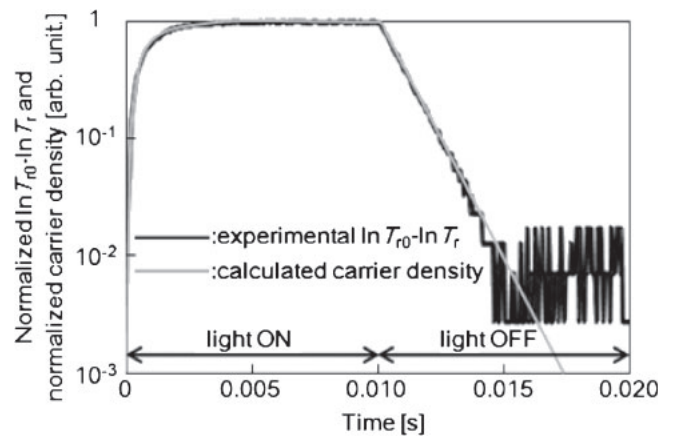


Fig. 10. Normalized difference in logarithm of the microwave transmittance between cases in the dark and under pulsed light illumination, $\ln T_{r0} - \ln T_r$, and normalized calculated change in carrier density per unit area given by eq. (9) during one period of light ON and OFF. The τ_{eff} measured by the present method with eq. (25) was 1.03×10^{-3} s.

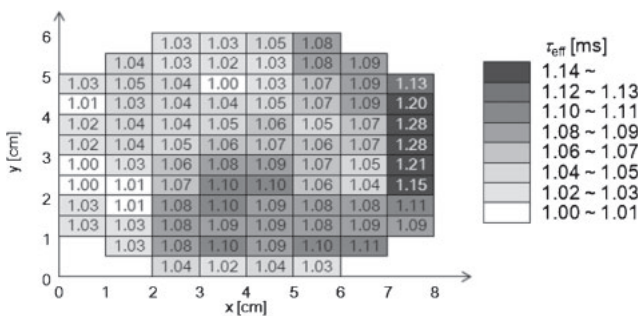


Fig. 9. τ_{eff} spatial distribution analyzed from $P(t)$ shown in Fig. 8 using eq. (25). τ_{eff} values were presented for each measurement point.

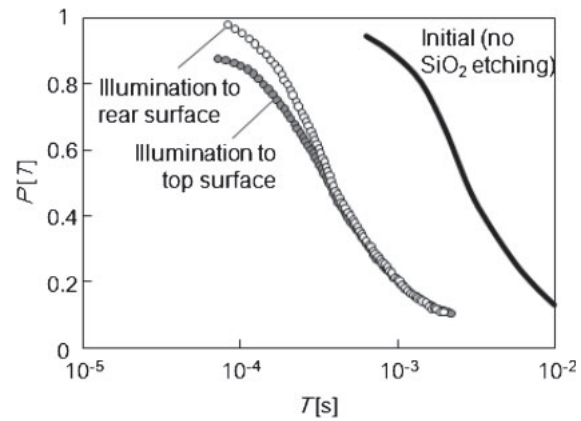


Fig. 11. $P(t)$ as a function of T for sample II in the cases of pulsed light illumination to the top surface with a 2-nm-thick SiO_2 layer and to the rear surface with a 100-nm-thick SiO_2 layer. $P(T)$ as a function of T for sample II, which was obtained prior to the SiO_2 etching, was also presented.

time resolution of 1×10^{-5} s. The present method made it possible to measure the minority carrier lifetime with a resolution of 1×10^{-5} s and a spatial resolution of about 1 cm under a low light intensity of 0.8 mW/cm^2 . One point of a sample was chosen to investigate a transient signal of microwave transmittance during light ON and OFF with a pulse width of 1×10^{-2} s using a digital oscilloscope. Figure 10 shows a normalized difference in the logarithm of the microwave transmittance between cases in the dark and under pulsed light illumination, $\ln T_{r0} - \ln T_r$, and a normalized calculated change in carrier density per unit area given by eq. (9) during one period of light ON and OFF. Prior to the measurement, a sufficient number of light pulses were irradiated to realize periodic changes in the minority carrier density, as shown in eq. (7). τ_{eff} measured by the present method with eq. (25) was 1.03×10^{-3} s. The logarithmic plot of the vertical axis of Fig. 10 clearly shows a single exponential decay of $\ln T_{r0} - \ln T_r$ since the light pulse was OFF although the noise level was rather high at 10^{-2} . Fitting a calculated curve to the experimental one resulted in a time constant of 1.06×10^{-3} s. This value well agreed with 1.03×10^{-3} s obtained by the present method.

Figure 11 shows $P(T)$ as a function of T for sample II in the cases of pulsed light illumination to the top surface with a 2-nm-thick SiO_2 layer and to the rear surface with a 100-nm-thick SiO_2 layer. Figure 11 also shows $P(T)$ as a function of T for sample II, which was obtained prior to the SiO_2 etching. The initial sample II had a high τ_{eff} of 1.05×10^{-3} s, which was very close to that of sample I. On

the other hand, $P(T)$ shifted to small-pulse-width regions in the case of the top surface with a 2-nm-thick SiO_2 layer. In the case of illumination to the top surface, $P(T)$ gradually decreased as T increased. On the other hand, it was almost 1 up to 8×10^{-5} s in the case of illumination to the rear surface. Then it rapidly decreased as T increased from 8×10^{-5} s. Such different behaviors of $P(T)$ for different means of light illumination were well explained by our theory discussed above. Experimental $P(T)$ was analyzed using our model as shown in Table I. τ_{eff} was high at 1.05×10^{-3} s for original sample II prior to the etching of SiO_2 . It markedly decreased to 7.0×10^{-5} and 1.73×10^{-4} s for light illuminations to the top surface and rear surface, respectively, when the SiO_2 layer was etched up to 2 nm at the top surface. Two different τ_{eff} values clearly indicate that the carrier annihilation property depends on the means of light illumination for a defective sample. The analysis of above three τ_{eff} values using eq. (3) resulted in the most possible τ_b , S_{top} and S_{rear} as 5.2×10^{-3} s, 680 cm/s, and 20 cm/s respectively, for sample II with a 2-nm-thick SiO_2 layer at the top surface. Etching the SiO_2 layer increased the

Table I. Experimental τ_{eff} , $\ln T_{r0} - \ln T_r$, and $(\ln T_{r0} - \ln T_r)\tau_{\text{eff}}^{-1}$ values for light illumination to the top surface and rear surface for sample II with 2-nm-thick SiO₂ layer at the top surface, and for light illumination to the rear surface for original sample II coated with 100-nm-thick SiO₂ layer.

	Illumination to top surface	Illumination to rear surface	Illumination to rear surface (initial)
τ_{eff} (s)	7.0×10^{-5}	1.73×10^{-4}	1.05×10^{-3}
$\ln T_{r0} - \ln T_r$	0.011	0.0263	0.1622
$(\ln T_{r0} - \ln T_r)\tau_{\text{eff}}^{-1}$ (s ⁻¹)	158	152	154

recombination velocity at the top surface. The experimental demonstrations of Figs. 8–10 show that the present method has a capability for the precise measurement of the minority carrier lifetime and defect localization properties under illumination with a low light intensity. We also measured the change in microwave transmissivity by CW light illumination at 0.8 mW/cm² for sample II. As described in eqs. (2) and (23), the carrier density per unit area during CW light illumination was proportional to the logarithm of the change in transmissivity by CW light illumination and the minority carrier lifetime as

$$N = \frac{1}{C} (\ln T_{r0} - \ln T_r) = \tau_{\text{eff}}^{\text{CW}} G. \quad (26)$$

The logarithms of the change in transmissivity by CW light illumination, $\ln T_{r0} - \ln T_r$, were 0.1622 for the original sample II with a 100-nm-thick SiO₂ layer in the case of light illumination to the rear surface. It decreased to 0.0263 for sample II with a 2-nm-thick SiO₂ layer at the top surface in the case of light illumination to the rear surface, as shown in Table I. The difference in the above two values must result from change in the effective carrier lifetime for CW light illumination caused by etching SiO₂ at the top surface because the rear surface maintained the same properties including the optical reflectivity property, which meant that G in eq. (26) remained constant. τ_{eff} obtained by the present method was 1.05×10^{-3} s for the original sample. It decreased to 1.73×10^{-4} s for sample II with a 2-nm-thick SiO₂ layer at the top surface in the case of light illumination to the rear surface. The values of $\ln T_{r0} - \ln T_r$ divided by τ_{eff} were almost the same between the cases of light illumination to the rear surface for the original sample II and sample II with a 2-nm-thick SiO₂ layer at the top surface. Those results mean that τ_{eff} given by eq. (25) is in good agreement with $\tau_{\text{eff}}^{\text{CW}}$.

5. Conclusions

We reported the measurement of the minority carrier lifetime of silicon using free-carrier absorption of 9.35 GHz microwaves under illumination with a low light intensity. We constructed a measurement system of photoinduced minority carrier absorption of 9.35 GHz microwaves using periodically pulsed light illumination at 620 nm at 0.8 mW/cm². We also developed a numerical analysis program of photoinduced carrier generation, diffusion, and annihilation at surfaces with S_{top} and S_{rear} and in the bulk substrate with τ_b . The ratio of the average carrier density when light illumination is ON to that when light illumination is OFF, $P(T)$, was introduced to investigate carrier annihilation

properties. $P(T)$ changed from 1 to 0 as the pulse width of light, T , increased. It simply changed with a single time constant τ_b when S_{top} and S_{rear} were zero. On the other hand, $P(T)$ remained almost 1 for T until a diffusion time in the substrate even when S_{rear} was very large if τ_b was large and S_{top} was zero. $P(t)$ decreased for a short T when S_{top} markedly increased. We introduced τ_{pulse} as a pulse width for $P(t)$ at 0.859 and R as a ratio of the difference between pulse widths for $P(t)$ at 0.615 and 0.859 to τ_{pulse} . We defined the effective minority carrier lifetime τ_{eff} using τ_{pulse} and R as $\tau_{\text{pulse}}/(1 + \log R)$. We demonstrated that τ_{eff} is in good agreement with the minority carrier lifetime over a wide range of τ_{eff} values for CW light illumination. It is possible to determine the minority carrier lifetime without information on the carrier generation rate including surface reflection loss using our method with τ_{eff} . $\tau_{\text{classical}}$ given as $(\tau_b^{-1} + S_{\text{top}}/d + S_{\text{rear}}/d)^{-1}$ coincided with τ_{eff} when τ_{eff} was above 4×10^{-4} and 2×10^{-4} s for hole and electron minority carriers, respectively, for a 520- μm -thick silicon substrate.

τ_{eff} for hole minority carriers was experimentally demonstrated for n-type silicon samples coated with 100-nm-thick thermally grown SiO₂ layers. The spatial distribution of τ_{eff} was obtained to be 1.0×10^{-3} to 1.28×10^{-3} s with a resolution of 1×10^{-5} s over a 4-in. substrate. When the SiO₂ layer was etched up to 2 nm at the top surface, we obtained two different τ_{eff} values of 7×10^{-5} and 1.73×10^{-4} s in the cases of light illumination to the top surface and rear surface, respectively. This demonstrated that minority carrier density depended on the means of light illumination for defective samples with a low τ_{eff} .

Acknowledgment

This work was partly supported by a Grant-in-Aid for Science Research C (No. 22560292) from the Ministry of Education, Culture, Sports, Science, and Technology of Japan.

- 1) A. Rohatagi: Proc 3rd World Conf. Photovoltaic Energy Conversion, 2003, p. A29.
- 2) M. A. Green: *Prog. Photovoltaics* **17** (2009) 183.
- 3) G. S. Kousik, Z. G. Ling, and P. K. Ajmera: *J. Appl. Phys.* **72** (1992) 141.
- 4) J. M. Borrego, R. J. Gutmann, N. Jensen, and O. Paz: *Solid-State Electron.* **30** (1987) 195.
- 5) G. W. 't Hooft, C. Van Oopdorp, H. Veenvliet, and A. T. Vink: *J. Cryst. Growth* **55** (1981) 173.
- 6) H. Daio and F. Shimura: *Jpn. J. Appl. Phys.* **32** (1993) L1792.
- 7) J. Sritharathikhun, C. Banerjee, M. Otsubo, T. Sugiura, H. Yamamoto, T. Sato, A. Limmanee, A. Yamada, and M. Konagai: *Jpn. J. Appl. Phys.* **46** (2007) 3296.
- 8) Y. Takahashi, J. Nigo, A. Ogane, Y. Uraoka, and T. Fuyuki: *Jpn. J. Appl. Phys.* **47** (2008) 5320.
- 9) M. Boulou and D. Bois: *J. Appl. Phys.* **48** (1977) 4713.
- 10) Y. Ogita: *J. Appl. Phys.* **79** (1996) 6954.
- 11) C. Munakata: *Jpn. J. Appl. Phys.* **43** (2004) L1394.
- 12) J. W. Orton and P. Blood: *The Electrical Characterization of Semiconductors: Measurement of Minority Carrier Properties* (Academic Press, London, 1990) Chap. 4.
- 13) T. Sameshima, H. Hayasaka, and T. Haba: *Jpn. J. Appl. Phys.* **48** (2009) 021204.
- 14) T. Sameshima, M. Shimokawa, J. Takenezawa, T. Nagao, M. Hasumi, S. Yoshidomi, N. Sano, and T. Mizuno: Proc. 6th Thin Film Materials and Devices Meet., 2009, p. 100228115.
- 15) A. S. Groove: *Physics and Technology of Semiconductor Devices* (Wiley, New York, 1967) Chap. 5.
- 16) E. D. Palk: *Handbook of Optical Constants of Solids* (Academic Press, London, 1985) p. 547.